Plasma formation and temperature measurement during single-bubble cavitation

David J. Flannigan & Kenneth S. Suslick

Department of Chemistry, University of Illinois at Urbana-Champaign, Urbana, Illinois 61801, USA

Single-bubble sonoluminescence (SBSL[1–5]) results from the extreme temperatures and pressures achieved during bubble compression; calculations have predicted[6,7] the existence of a hot, optically opaque plasma core[8] with consequent bremsstrahlung radiation[9,10]. Recent controversial reports[11,12] claim the observation of neutrons from deuterium–deuterium fusion during acoustic cavitation[11,12]. However, there has been previously no strong experimental evidence for the existence of a

plasma during single- or multi-bubble sonoluminescence. SBSL typically produces featureless emission spectra[13] that reveal little about the intra-cavity physical conditions or chemical processes. Here we report observations of atomic (Ar) emission and extensive molecular (SO) and ionic (O_2^+) progressions in SBSL spectra from concentrated aqueous H_2SO_4 solutions. Both the Ar and SO emission permit spectroscopic temperature determinations, as accomplished for multi-bubble sonoluminescence with other emitters[14–16]. The emissive excited states observed from both Ar and O_2^+ are inconsistent with any thermal process. The Ar excited states involved are extremely high in energy (>13 eV) and cannot be thermally populated at the measured Ar emission temperatures (4,000–15,000 K); the ionization energy of O_2 is more than twice its bond dissociation energy, so O_2^+ likewise cannot be thermally produced. We therefore conclude that these emitting species must originate from collisions with high-energy electrons, ions or particles from a hot plasma core.

In order to gain insight into the physical conditions and chemical processes occurring during single-bubble cavitation, we have explored a variety of low-volatility liquids[17], observing both stationary and moving SBSL. We have now discovered the generation of extremely intense SBSL from a moving single bubble in concentrated aqueous H_2SO_4 solutions, H_2SO_4(aq.), which have very low vapour pressures[18] and are essentially transparent down to a wavelength of 200 nm. Under optimal conditions, the SBSL intensity from 85 wt% H_2SO_4(aq.) under Ar is increased 2,700 times compared to that from water under Ar, and the intensity under Xe is increased 1,500 times compared to water under Xe (Fig. 1). When Xe is dissolved in degassed 85% H_2SO_4(aq.), the SBSL is, by more than two orders of magnitude, the most intense yet observed in any liquid. SBSL from H_2SO_4 solutions had been previously reported, but with only a few-fold increase in intensity compared to water[19].

Bright SBSL spectra from concentrated H_2SO_4(aq.) are similar to water SBSL spectra, consisting of a featureless continuum that increases towards the ultraviolet (UV). Although these spectra are much more intense, blackbody fits (which have been previously reported for SBSL in water[20]) do not yield vastly different temperatures for the SBSL now observed from H_2SO_4(aq.); all four spectra in Fig. 1 have an apparent blackbody temperature of ~12,500 ± 1,500 K. The very marked increase in SBSL intensity seen from concentrated H_2SO_4(aq.) is due in part to the much lower concentration of polyatomic species inside the bubble relative to water at the same temperature: less of the energy of cavitation is consumed by endothermic bond dissociations[21]. The remaining bubble contents, comprised almost entirely of noble gas atoms mixed with a small amount of H_2SO_4 vapour, must therefore absorb a larger portion of the energy of collapse.

Importantly, the parameter space that supports SBSL in H_2SO_4(aq.) is much larger than in water, with SBSL observable over an acoustic pressure range of 1.3 to >6 bar. (The acoustic pressures are estimated from hydrophone measurements at the centre of the acoustic field; movement of the bubble about the

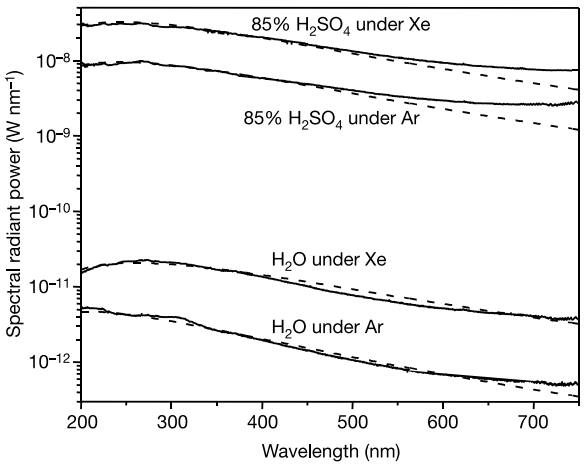

Figure 1 SBSL spectra from 85% H_2SO_4(aq.) and pure water regassed with Xe and Ar (solid lines); apparent fits to blackbody spectra are given as dashed lines. Noble gas content of solutions, acoustic frequency and acoustic pressure were adjusted to obtain the brightest SBSL emission. The SBSL apparatus, spectral acquisition system and acoustic pressure measurements have been previously described[17]. All spectra were corrected for solution and resonator absorption, and for the response of the optical system (against NIST traceable standard lamps).

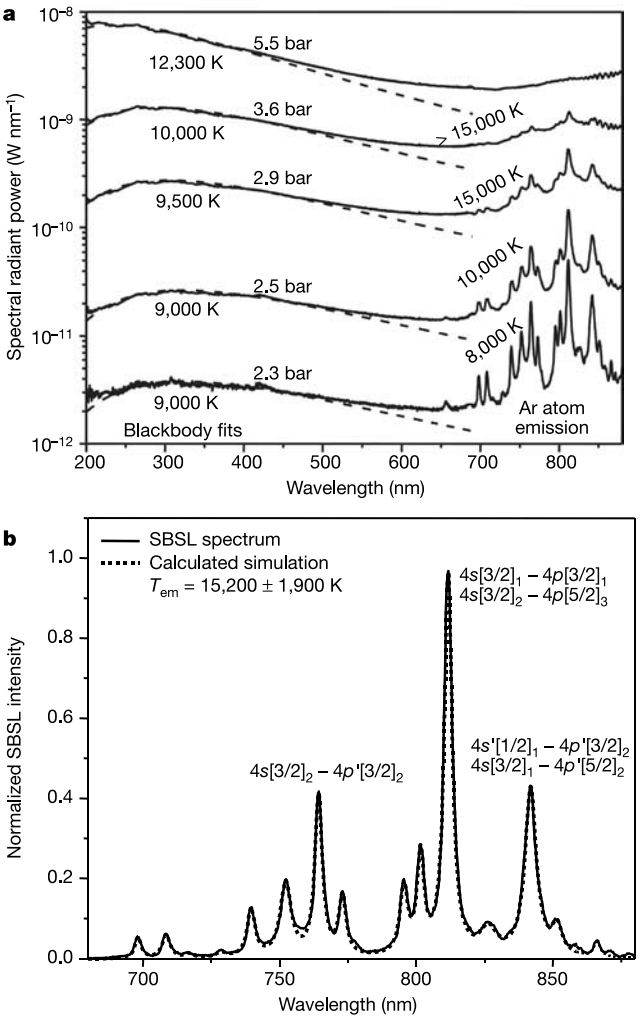

Figure 2 SBSL spectra from 85% H_2SO_4(aq.). **a**, Solid lines are the observed SBSL emission spectra, dashed lines are calculated blackbody spectra. Applied acoustic pressures are shown above their corresponding plot. Temperatures of blackbody fits and of Ar atom emission (compare with **b**) are shown next to their corresponding plot. The strong neutral Ar atom emission lines in the red and near-infrared region of the spectra arise from the 4*s*–4*p* manifold. The 4*s* state is situated 11.5–11.8 eV above the ground state (3*p*), whereas the 4*p* state lies 13.1–13.5 eV above the ground state. **b**, Ar atom line emission (2.8 bar; solid line) compared to a calculated Ar atom emission spectrum at 15,200 K (dashed line). The underlying continuum has been subtracted; spectra are normalized to intensity at 811 nm. The most prominent lines are labelled with the corresponding transitions. The lines at 811 and 840 nm each contain contributions from two relatively strong transitions.

pressure antinode will decrease the effective acoustic pressure experienced by the bubble, so acoustic pressures given here are upper limits.) In SBSL from more weakly driven bubbles, for example, we observe very strong atomic emission from neutral Ar (Fig. 2). In this case, as the driving acoustic pressure is increased, the intensity of Ar emission lines decreases relative to the continuum emission, and the Ar lines broaden gradually into unresolved peaks at >5 bar. Observation of emission from excited states of atomic Ar allows us to calculate emission temperatures from the well-known energy levels, transition probabilities, statistical weights, and photon energies of Ar (ref. 22). Ar atom emission temperatures generated during SBSL from 85% H_2SO_4(aq.) were observed to increase with increasing acoustic pressure, and were found to be 8,000 ± 1,000 K at 2.3 bar, 10,700 ± 1,300 K at 2.5 bar, and 15,200 ± 1,900 K at 2.8 bar. Note that these experimentally determined temperatures are consistent with theoretically predicted SBSL temperatures[7,23]. At higher acoustic pressures, accurate fits to Ar emission spectra become difficult owing to line broadening and the development of line asymmetries, possibly due to increased Ar ion concentrations. At the highest acoustic pressures reached before the bubble was forced from the centre of the resonator (>6 bar), calculation of SBSL temperature was impossible owing to the extreme broadening of all spectral features.

We note especially that the Ar excited states that are being populated are extremely high in energy (>13 eV)[24], which is too high to be populated thermally at the <1 eV effective emission temperature of Ar. This provides, to our knowledge, the first experimental evidence for excitation via high-energy particle collisions (for example, electron impact on Ar) from a hot plasma core. The possibility of an optically opaque, highly ionized plasma core during SBSL has been previously suggested by calculations[8]. Similar circumstances occur during intense shockwave heating in gases. For example, the limiting emission temperature of an intense shockwave in air is only ~17,000 K (ref. 25), which represents the opacity limit of shock heating of air, and shock-heated Ar plasmas typically have line emission temperatures below ~20,000 K (ref. 26).

Comparisons of Ar atom emission temperatures to blackbody fits of the UV continuum (Figs 1 and 2a) are problematic for several reasons. First, the origin of the UV continuum emission is unclear: it may be partially blackbody radiation from the emitting shell surrounding an optically opaque core[6,7], and partially bremsstrahlung due to ionization[9,10,27]. It could also be due to ion–electron recombination, which is likely to be present in a dense plasma[9,10]. Furthermore, the continuum emission and the well-resolved Ar atom emission do not necessarily originate at the same time during bubble collapse or from the same spatial region within the bubble. A simple blackbody fit under these circumstances is unlikely to produce an accurate temperature measurement, and further comparison is therefore unwarranted.

According to current theoretical models of SBSL, compressional heating of the bubble should show some dependence on the thermal conductivity of the gas within the bubble[23,28]. As shown in Fig. 3, we can use mixtures of Ar and Ne to systematically control the emission temperature from >15,000 K down to ~1,500 K. The effects of thermal conductivity may come both from direct thermal transport and from changes in the size of the plasma core[8,23,25]. Thus it is clear that bubble collapse is only approximately adiabatic, and that even in SBSL, thermal conductivity of the dissolved gases is a critical experimental parameter.

We also observe extensive vibronic progressions arising from the $B^3\Sigma^- – X^3\Sigma^-$ system of sulphur monoxide (SO; ref. 29) in the SBSL spectra of concentrated H_2SO_4(aq.). Sulphur monoxide vibronic progressions are most prominent when the H_2SO_4(aq.) solution contains dissolved Ne (Fig. 4a). The bands are very weakly present in SBSL spectra of a very dimly luminescing Ar bubble, and they are totally absent from SBSL spectra of Kr and Xe bubbles, no matter how dim. If heat is rapidly conducted out of a Ne-filled bubble during collapse, dissociation of SO will occur to a lesser degree, resulting in an increase in SO emission intensity, as observed.

By comparing relative intensities of inter-progression SO emission bands, and also by observing how relative intensities of the bands change with increasing acoustic pressure, effective SO temperatures were determined to be 1,580 ± 110 K at 3.3 bar, 2,470 ± 170 K at 4.2 bar, and 3,480 ± 240 K at 5.1 bar, all regassed with Ne. At higher acoustic pressures, the emission temperatures continue to increase and become difficult to determine, owing to the blending of bands and the decrease in SO emission intensity (as dissociation occurs). Note that at the highest acoustic pressures applied (>6 bar), features of SO molecular emission were still apparent in the spectra. Emission temperatures from SO are of course limited by its dissociation, and so may represent either

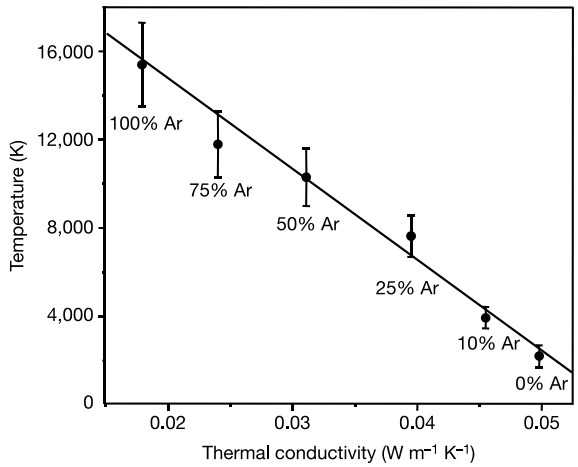

Figure 3 Emission temperatures of SBSL of 85% H_2SO_4(aq.) regassed with Ar/Ne mixtures (acoustic pressure 3 bar) are shown as a function of the thermal conductivity of the gas mixtures. Temperatures were calculated from Ar atom emission for all but the 100% Ne measurement, whose temperature was determined from SO emission (compare Fig. 4). Error bars are determined from the errors in the transition probabilities reported in ref. 20, and from an estimated 5% experimental error in the measured temperature.

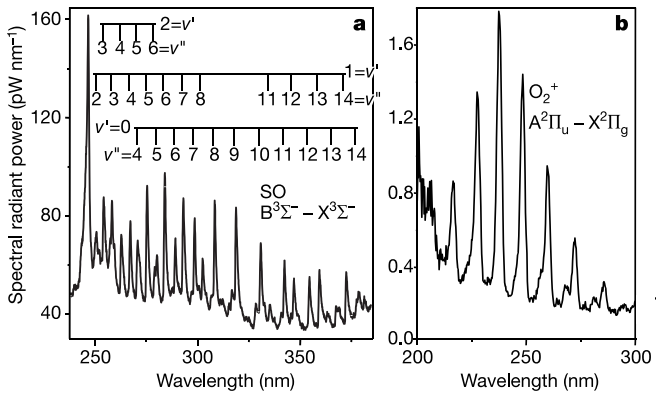

Figure 4 Vibronic progressions in SBSL spectra. **a**, Sulphur monoxide (SO) ($B^3\Sigma^- – X^3\Sigma^-$) emission from 85% H_2SO_4(aq.) regassed with Ne. The intense peak near 250 nm arises from the SO ultraviolet system ($A^3\Pi – X^3\Sigma^-$; ref. 29). Vibrational levels in the $B^3\Sigma^-$ state are denoted by v' while vibrational levels in the $X^3\Sigma^-$ state are denoted by v''. **b**, Dioxygenyl cation (O_2^+) ($A^2\Pi_u – X^2\Pi_g$) emission[30] from 85% H_2SO_4(aq.) regassed with O_2/Xe.

emission from outer regions of the collapsing bubble or early (or late) times during bubble collapse.

Confirmation of the presence of a plasma in the collapsing bubble comes from the observation of O_2^+ emission[30] (Fig. 4b). The bond energies of O_2 and O_2^+ are 5.1 and 6.5 eV, respectively, while the ionization energy of O_2 is much higher at 12.1 eV. A total of over 18 eV of energy is necessary to form excited O_2^+. The formation and excitation of O_2^+ therefore cannot occur thermally, and probably occurs via high-energy electron impact from the hot, opaque plasma core. To our knowledge, this is the first example of emission from any ion in any sonoluminescence spectrum under any conditions. □

Received 15 September 2004; accepted 17 January 2005; doi:10.1038/nature03361.

1. Barber, B. P. & Putterman, S. J. Light scattering measurements of the repetitive supersonic implosion of a sonoluminescing bubble. *Phys. Rev. Lett.* **69,** 3839–3842 (1992).
2. Gompf, B., Günther, R., Nick, G., Pecha, R. & Eisenmenger, W. Resolving sonoluminescence pulse width with time-correlated single photon counting. *Phys. Rev. Lett.* **79,** 1405–1408 (1997).
3. Gaitan, D. F., Crum, L. A., Church, C. C. & Roy, R. A. Sonoluminescence and bubble dynamics for a single, stable, cavitation bubble. *J. Acoust. Soc. Am.* **91,** 3166–3183 (1992).
4. Lohse, D., Brenner, M. P., Dupont, T. F., Hilgenfeldt, S. & Johnston, B. Sonoluminescing air bubbles rectify argon. *Phys. Rev. Lett.* **78,** 1359–1362 (1997).
5. Brenner, M. P., Hilgenfeldt, S. & Lohse, D. Single-bubble sonoluminescence. *Rev. Mod. Phys.* **74,** 425–484 (2002).
6. Moss, W. C., Clarke, D. B. & Young, D. A. Calculated pulse widths and spectra of a single sonoluminescing bubble. *Science* **276,** 1398–1401 (1997).
7. Moss, W. C. *et al.* Computed optical emissions from a sonoluminescing bubble. *Phys. Rev. E* **59,** 2986–2992 (1999).
8. Burnett, P. D. S. *et al.* Modeling a sonoluminescing bubble as a plasma. *J. Quant. Spectrosc. Radiat. Transfer* **71,** 215–223 (2001).
9. Hilgenfeldt, S., Grossmann, S. & Lohse, D. A simple explanation of light emission in sonoluminescence. *Nature* **398,** 402–405 (1999).
10. Yasui, K. Mechanism of single-bubble sonoluminescence. *Phys. Rev. E* **60,** 1754–1758 (1999).
11. Taleyarkhan, R. P. *et al.* Evidence for nuclear emissions during acoustic cavitation. *Science* **295,** 1868–1873 (2002).
12. Taleyarkhan, R. P. *et al.* Additional evidence of nuclear emissions during cavitation. *Phys. Rev. E* **69,** 036109 (2004).
13. Hiller, R., Weninger, K., Putterman, S. J. & Barber, B. P. Effect of noble gas doping in single-bubble sonoluminescence. *Science* **266,** 248–250 (1994).
14. McNamara, W. B. III, Didenko, Y. T. & Suslick, K. S. Sonoluminescence temperatures during multi-bubble cavitation. *Nature* **401,** 772–775 (1999).
15. Flint, E. B. & Suslick, K. S. The temperature of cavitation. *Science* **253,** 1397–1399 (1991).
16. Didenko, Y. T., McNamara, W. B. III & Suslick, K. S. Effect of noble gases on sonoluminescence temperatures during multibubble cavitation. *Phys. Rev. Lett.* **84,** 777–780 (2000).
17. Didenko, Y. T., McNamara, W. B. III & Suslick, K. S. Molecular emission from single-bubble sonoluminescence. *Nature* **407,** 877–879 (2000).
18. Greenewalt, C. H. Partial pressures of aqueous solutions of sulfuric acid. *J. Ind. Eng. Chem.* **17,** 522–523 (1925).
19. Troia, A., Ripa, D. M. & Spagnolo, R. in *World Congress on Ultrasonics* (ed. Cassereau, D.) 1041–1044 (Société Française d'Acoustique, Paris, 2003).
20. Vazquez, G., Camara, C., Putterman, S. & Weninger, K. Sonoluminescence: Nature's smallest blackbody. *Opt. Lett.* **26,** 575–577 (2001).
21. Didenko, Y. T. & Suslick, K. S. The energy efficiency of formation of photons, radicals and ions during single-bubble cavitation. *Nature* **418,** 394–397 (2002).
22. Wiese, W. L., Brault, J. W., Danzmann, K., Helbig, V. & Kock, M. Unified set of atomic transition probabilities for neutral argon. *Phys. Rev. A.* **39,** 2461–2471 (1989).
23. Toegel, R. & Lohse, D. Phase diagrams for sonoluminescing bubbles: A comparison between experiment and theory. *J. Chem. Phys.* **118,** 1863–1875 (2003).
24. Cooper, R., Grieser, F., Sauer, M. C. Jr & Sangster, D. F. Formation and decay kinetics of the 2p levels of neon, argon, krypton, and xenon produced by electron-beam pulses. *J. Phys. Chem.* **81,** 2215–2220 (1977).
25. Zel'dovich, Y. B. & Raizer, Y. P. *Physics of Shock Waves and High-Temperature Hydrodynamic Phenomena* (Academic, New York, 1966).
26. Tourin, R. H. *Spectroscopic Gas Temperature Measurement* (Elsevier, Amsterdam, 1966).
27. Camara, C., Putterman, S. & Kirilov, E. Sonoluminescence from a single bubble driven at 1 megahertz. *Phys. Rev. Lett.* **92,** 124301 (2004).
28. Yasui, K. Single-bubble sonoluminescence from noble gases. *Phys. Rev. E* **63,** 035301 (2001).
29. Ajello, J. M. *et al.* Middle ultraviolet and visible spectrum of SO_2 by electron impact. *J. Geophys. Res. Space* **107,** SIA2 (2002).
30. Schappe, R. S., Schulman, M. B., Sharpton, F. A. & Lin, C. C. Emission of the O_2^+ ($A^2\Pi_u \rightarrow X^2\Pi_g$) second-negative-band system produced by electron impact on O_2. *Phys. Rev. A* **38,** 4537–4545 (1988).

Acknowledgements This work was supported by the National Science Foundation and the US Defense Advanced Research Projects Agency. We acknowledge conversations with F. Grieser on the mechanism of Ar atom emission, and with L. A. Crum, D. Lohse, W. C. Moss and S. J. Putterman.

Competing interests statement The authors declare that they have no competing financial interests.

Correspondence and requests for materials should be addressed to K.S.S. (ksuslick@uiuc.edu).